Hydrogel-based delivery of antimiR-221 enhances cartilage regeneration by endogenous cells

Andrea Lolli[a], Kavitha Sivasubramaniyan[a], Maria L. Vainieri[a,b], Jacopo Oieni[c], Nicole Kops[a], Avner Yayon[d], Gerjo J.V.M. van Osch[a,e,*]

[a] Department of Orthopaedics, Erasmus MC, University Medical Center, Rotterdam, the Netherlands
[b] AO Research Institute, Davos, Switzerland
[c] Faculty of Biotechnology and Food Engineering, Technion - Israel Institute of Technology, Haifa, Israel
[d] ProCore Ltd., Weizmann Science Park, Nes Ziona, Israel
[e] Department of Otorhinolaryngology, Head and Neck Surgery, Erasmus MC, University Medical Center, Rotterdam, the Netherlands

ARTICLE INFO

ABSTRACT

Articular cartilage is frequently injured by trauma or osteoarthritis, with limited and inadequate treatment options. We investigated a new strategy based on hydrogel-mediated delivery of a locked nucleic acid microRNA inhibitor targeting miR-221 (antimiR-221) to guide *in situ* cartilage repair by endogenous cells.

First, we showed that transfection of antimiR-221 into human bone marrow-derived mesenchymal stromal cells (hMSCs) blocked miR-221 expression and enhanced chondrogenesis *in vitro*. Next, we loaded a fibrin/hyaluronan (FB/HA) hydrogel with antimiR-221 in combination or not with lipofectamine carrier. FB/HA strongly retained functional antimiR-221 over 14 days of *in vitro* culture, and provided a supportive environment for cell transfection, as validated by flow cytometry and qRT-PCR analysis. Seeding of hMSCs on the surface of antimiR-221 loaded FB/HA led to invasion of the hydrogel and miR-221 knockdown *in situ* within 7 days. Overall, the use of lipofectamine enhanced the potency of the system, with increased antimiR-221 retention and miR-221 silencing in infiltrating cells. Finally, FB/HA hydrogels were used to fill defects in osteochondral biopsies that were implanted subcutaneously in mice. FB/HA loaded with antimiR-221/lipofectamine significantly enhanced cartilage repair by endogenous cells, demonstrating the feasibility of our approach and the need to achieve highly effective *in situ* transfection.

Our study provides new evidence on the treatment of focal cartilage injuries using controlled biomaterial-mediated delivery of antimicroRNA for *in situ* guided regeneration.

1. Introduction

The repair of articular cartilage damaged by trauma or osteoarthritis represents an unmet clinical need. When conservative management is no longer possible, surgical interventions including microfracture and osteochondral grafting are considered. Unfortunately, these procedures do not lead to the production of long-lasting functional hyaline cartilage. Encouragingly, cell-based therapies have emerged as a new opportunity. Autologous chondrocyte implantation (ACI) was shown to be superior to microfracture for treating cartilage defects after a 5-year follow-up [1]. Transplantation of human mesenchymal stromal cells (hMSCs) is at an earlier stage, but phase I/II clinical trials have proved its safety and therapeutic potential [2–4]. Nevertheless, the implementation of cell therapy into clinical practice is

facing several hurdles, due to the extensive cost and time required for *in vitro* cell manipulation, as well as regulatory issues related to safety and quality control [5].

The formation of cartilaginous tissue following microfracture surgery indicates that cartilage repair can be achieved by directly stimulating joint-resident progenitor cells *in situ* [6]. Perforation of the subchondral bone induces a healing response where bone marrow-resident cells access the lesion and trigger repair. Previous studies confirmed that progenitor cells in the bone marrow and in the synovium can migrate towards the sites of cartilage damage and initiate the repair of partial or full-thickness cartilage defects [7,8]. Unfortunately, the repair tissue produced after microfracture is mainly of fibrocartilaginous nature and was shown to undergo deterioration within 2 years of surgery [9]. To address these concerns, the combination of microfracture

---

with the implantation of a scaffold or a hydrogel was proposed, as in the case of the autologous matrix-induced chondrogenesis approach using a collagen membrane [10], or the BST-CarGel approach using a chitosan hydrogel and autologous blood [11]. Besides providing structural support and a scaffold for progenitor cells to colonize the defect, this could enable the delivery of bioactive molecules to improve endogenous repair. In this context, the development of matrices loaded with gene constructs is an attractive option to deliver therapeutics and orient the fate of progenitor cells *in situ* (*e.g.* [12–15]). Such an approach could circumvent the issues of cell therapy and have an easier path to the clinic.

In recent years, the characterization of chondro-regulatory microRNAs (miRNAs) has reshaped our understanding of the control of cartilage homeostasis. miRNAs are small non-coding RNAs that regulate gene expression by base-pairing with complementary mRNAs and inhibiting their translation. miRNAs are major regulators of osteo-chondrogenic differentiation of progenitor cells and represent highly attractive targets for stimulating osteochondral repair [16–18]. Implantation of microRNA-transfected cells in combination with supportive scaffolds was previously shown to improve osteochondral repair *in vivo* (reviewed in [15]). Nevertheless, only few initial studies have investigated the use of miRNA-loaded collagen-based scaffolds to stimulate bone repair by endogenous cells [12,19]. In the field of cartilage repair, the possibility to employ miRNA-loaded matrices to stimulate endogenous healing is still uncharted territory.

We previously characterized miR-221 as novel anti-chondrogenic miRNA, and found that silencing miR-221 in cultured bone marrow-derived hMSCs induced chondrogenesis [20,21]. Implantation of miR-221 depleted hMSCs in a cartilage defect model significantly enhanced cartilage repair *in vivo* [21]. Thus, we hypothesized that silencing miR-221 in endogenous progenitor cells could stimulate cartilage repair.

With the aim to develop such a strategy, we here loaded a fibrin/hyaluronan (FB/HA) hydrogel with a locked nucleic acid (LNA)-microRNA inhibitor against miR-221 (antimiR-221), with or without lipofectamine carrier. We performed *in vitro* studies to investigate the ability of the constructs to retain antimiR-221 and deliver it to bone marrow-derived stromal cells infiltrating the hydrogels. We then exploited an *in vivo* osteochondral defect model to test the ability of antimiR-221 loaded FB/HA to stimulate endogenous cartilage repair.

2. Materials and methods

2.1. Hydrogel preparation and loading with LNA-antimiR oligonucleotides

A FB/HA conjugate hydrogel (RegenoGel™) [22] was kindly provided by ProCore Biomed Ltd. (Nes Ziona, IL). The conjugate is composed of FB and HA in a 3.2:1 ratio, with a final concentration of 6.25 mg/mL FB and 1.95 mg/mL HA. In comparison to hydrogels prepared from FB alone or from a mixture of FB and HA, FB/HA conjugate hydrogels show enhanced stability and mechanical properties, with reduced loss of water and shrinkage overtime, as well as more pronounced viscoelastic properties [22].

FB/HA hydrogel constructs for *in vitro* cultures were prepared by mixing 150 μL of FB/HA conjugate with 10 μL of 50 U/mL thrombin (Sigma-Aldrich). When required, hMSCs were resuspended in the hydrogels prior to the addition of thrombin at a low concentration (3.5×10^6 cells/mL, in analogy to previous reports [22]). The hydrogels were allowed to polymerize at 37 °C for 30 min in 96-well culture plates, then removed from the plates and used for the experiments.

To prepare antimiR-loaded hydrogels, FB/HA was loaded with the indicated concentrations of miRCURY LNA miRNA Power Inhibitor "in vivo ready" against miR-221-3p (antimiR-221; QIAGEN), 6-FAM 5′-labelled miRCURY LNA miRNA Power Inhibitor against miR-221-3p (fluorescently labelled antimiR-221; QIAGEN) or miRCURY LNA miRNA Power Inhibitor "*in vivo* ready" mismatch scramble control (antimiR-Scr; QIAGEN), prior to polymerization. These chemically-

modified oligonucleotides contain LNA bases and a phosphorothioate backbone that can stimulate the process of gymnotic delivery [23]. "In vivo ready" refers to the purification of the inhibitors with standards suitable for *in vivo* delivery, *i.e.* HPLC and Na + salt exchange. For carrier-assisted transfection, Lipofectamine® RNAiMAX Reagent (ThermoFisher Scientific) was used as delivering agent and pre-incubated with antimiR-221 or antimiR-Scr and Opti-MEM Reduced Serum Medium (ThermoFisher Scientific) for 20 min at room temperature, following the manufacturer's instructions.

Collagen I hydrogels were prepared by mixing on ice 1.2 mg/mL collagen I (from rat tail; ThermoFisher Scientific) with $10 \times$ phosphate buffered saline (PBS), distilled water and 1 N NaOH. Similarly to FB/HA, the hydrogels were loaded with hMSCs and/or antimiR-221 and polymerized at 37 °C in culture plates until firm constructs were formed (30–40 min).

2.2. Analysis of antimiR-221 retention by FB/HA hydrogels

FB/HA hydrogels were loaded with 4 μM fluorescently labelled antimiR-221 with or without Lipofectamine® RNAiMAX Reagent. 100 μL hydrogel constructs were polymerized in 96-well plates, as described. 200 μL of PBS $1 \times$ were added on top of the hydrogels and the plates were incubated at 37 °C in a humidified atmosphere of 5% CO$_2$, up to 14 days. At every indicated time-point, the releasates were collected and replaced with fresh PBS. At the end of the experiment, the hydrogels were enzymatically digested with 2 mg/mL collagenase B (Sigma-Aldrich) in PBS at 37 °C for 90 min to retrieve the fraction of antimiR-221 that was still retained by the hydrogels. The antimiR-221 content of the samples was quantified by measuring the fluorescent signal at λ = 518 nm with a Spectramax microplate reader (Molecular Devices, CA, USA). The cumulative release of antimiR-221 from the hydrogels was determined following interpolation with a standard curve. The experiments were performed with triplicate samples.

2.3. hMSC isolation and culture

hMSCs were isolated from the femoral biopsies of donors (age 50–78 years) undergoing total hip replacement, after signed informed consent and approval of the local ethical committees (Erasmus MC METC-2015-644; Albert Schweizer Hospital 2011.07). Cells were seeded at a density of 5×10^4 nucleated cells/cm^2 in expansion medium (10% Fetal Calf Serum α-MEM (ThermoFisher Scientific) supplemented with 1 ng/mL FGF2 (AbD Serotec), 25 μg/mL ascorbic acid-2-phosphate (Sigma-Aldrich), 1.5 μg/mL fungizone, and 50 μg/mL gentamicin), at 37 °C in a humidified atmosphere of 5% CO$_2$. After 24 h, non-adherent cells were washed off. At subconfluence, adherent hMSCs were trypsinized and replated at a density of 2.3×10^3 cells/cm^2. The culture medium was refreshed twice a week and expanded cells at passage 2 to 4 were used for the experiments.

To confirm the functionality of antimiR-221, hMSCs cultured in monolayer were transfected with 5–50 nM antimiR-221, with or without lipofectamine. The transfected cells were cultured in 10% Fetal Calf Serum α-MEM (ThermoFisher Scientific) supplemented with 25 μg/mL ascorbic acid-2-phosphate (Sigma-Aldrich), 1.5 μg/mL fungizone, and 50 μg/mL gentamicin for 3 days at 37 °C in a humidified atmosphere of 5% CO$_2$, prior to RNA isolation. In order to test antimiR-221 stability over time, 250 nM antimiR-221 with or without lipofectamine in PBS was pre-incubated at 37 °C for 14 days, prior to hMSC transfection. The transfected cells were cultured for 3 days at 37 °C in a humidified atmosphere of 5% CO$_2$, prior to RNA isolation.

To assess the effect of antimiR-221 on chondrogenesis, hMSCs cultured in monolayer were transfected twice with 25 nM antimiR-221, as previously described [21]. hMSCs were then seeded in 15 mL-polypropylene conical tube and centrifuged to form 3D pellets (2×10^5 cells/pellet). The pellets were cultured in DMEM-high-glucose GlutaMAX+ (GIBCO) supplemented with 1% ITS+, 40 μg/mL L-proline

(Sigma-Aldrich), 1 mM sodium pyruvate (GIBCO), 100 nM dexamethasone (Sigma-Aldrich), 1.5 μg/mL fungizone, 50 μg/mL gentamicin and 10 ng/mL Transforming Growth Factor β1 (TGF-β1; R&D Systems) for 28 days. The culture medium was renewed twice a week.

To confirm the ability of hMSCs to undergo chondrogenesis in FB/HA, hydrogels were loaded with hMSCs and polymerized as described in the previous paragraph. The hydrogels were cultured in chondro-permissive medium (DMEM-high-glucose GlutaMAX+ (GIBCO), 1% ITS+, 40 μg/mL L-proline (Sigma-Aldrich), 1 mM sodium pyruvate (GIBCO), 100 nM dexamethasone (Sigma-Aldrich), 1.5 μg/mL fungizone, and 50 μg/mL gentamicin) containing 0.0875 IU/mL aprotinin (Sigma-Aldrich) and supplemented or not with 10 ng/mL Transforming Growth Factor β1 (TGF-β1; R&D Systems) to stimulate chondrogenesis, for 28 days. The culture medium was renewed twice a week.

2.4. Transfection of hMSCs in antimiR-loaded FB/HA hydrogels

To evaluate the ability of FB/HA to support cell transfection, hMSCs were resuspended in FB/HA loaded with antimiR-221 with lipofectamine. Hydrogel constructs were formed in duplicates or triplicates as previously described and cultured in chondro-permissive medium containing 0.0875 IU/mL aprotinin for 7 days, with a medium renewal twice per week. For the assessment of transfection efficiency, the hydrogels were enzymatically digested with 2 mg/mL collagenase B (Sigma-Aldrich) in PBS at 37 °C for 90 min. Next, α-MEM medium supplemented with 10% FCS was added and samples were centrifuged for 8 min at 400 g. Cell pellets were resuspended in PBS and the cell suspensions were filtered with 70 μm strainers. Flow cytometry analysis was performed to quantify the % of hMSCs transfected with fluorescently labelled antimiR-221 using BD FACSCanto II (BD Biosciences, CA, USA). Data were analyzed using BD FACSDiva software (BD Biosciences, CA, USA). For the assessment of miR-221 silencing, the hydrogels were manually homogenized and subjected to RNA isolation.

To assess the possibility to silence cells that invade a hydrogel, 200 μL hydrogel FB/HA constructs loaded with antimiR with or without lipofectamine were polymerized in 48-well plates in duplicates or triplicates as described above. 5 × 10^5 hMSCs were seeded on top of the hydrogels in 200 μL of 10% Fetal Calf Serum α-MEM (ThermoFisher Scientific) supplemented with 1 ng/mL FGF2 (Bio-Rad, UK), 25 μg/mL ascorbic acid-2-phosphate (Sigma-Aldrich), 1.5 μg/mL fungizone, and 50 μg/mL gentamicin. Cells were allowed to adhere for 1 h, before adding 300 μL of medium. The hydrogels were cultured for 7 days with a medium renewal on day 3, prior to RNA isolation to assess miR-221 silencing. In order to test antimiR-221 stability in FB/HA, hydrogels loaded with antimiR-221 with or without lipofectamine were pre-incubated at 37 °C for 14 days, prior to hMSC seeding. Following cell seeding, the hydrogels were further cultured for 7 days with a medium renewal on day 3, prior to RNA isolation.

2.5. Analysis of hMSC viability in FB/HA hydrogels

To measure hMSC viability in FB/HA hydrogels, AlamarBlue Cell Viability assay (ThermoFisher Scientific) was performed at day 7 and 14 of culture. Briefly, AlamarBlue was added in the culture medium at a volume ratio of 1:10 and incubated for 8 h at 37 °C. Next, light absorbance at 570 nm and 600 nm was measured using a Spectramax microplate reader (Molecular Devices, CA, USA), according to the manufacturer's instructions. Results were normalized to medium control and expressed as % of AlamarBlue reduction.

2.6. RNA isolation and qRT-PCR

FB/HA hydrogels and hMSC pellets were manually homogenized in 700 μL of QIAzol Lysis Reagent (QIAGEN) and total RNA including miRNAs was purified using the miRNeasy Micro Kit (QIAGEN), according to the manufacturer's instructions. RNA concentration and

quality was determined using a NanoDrop ND1000 UV-VIS spectrophotometer (ThermoFisher Scientific). cDNA was synthesized from total RNA in a 20 μL reaction volume using the TaqMan MicroRNA Reverse Transcription kit (ThermoFisher Scientific) for the analysis of microRNAs, or the RevertAid First Strand cDNA synthesis kit (MBI Fermentas) for the analysis of mRNAs.

Quantification of miR-221-3p was performed with TaqMan MicroRNA Assays (ThermoFisher Scientific), using U6 snRNA for normalization. For the analysis of expression of genes indicative for chondrogenic differentiation, collagen II, aggrecan and collagen X were used, with hypoxanthine-guanine phosphoribosyltransferase (HPRT) gene for normalization of mRNA abundances. Polymerase chain reactions were performed using the TaqMan Universal PCR MasterMix (ThermoFisher Scientific) and the CFX96TM PCR detection system (Bio-Rad). Relative gene expression was calculated using the comparative $2^{-\Delta Ct}$ method.

2.7. RNA-sequencing and bioinformatic analysis

To assess the effect of miR-221 silencing on gene expression, hMSCs cultured in monolayer were transfected with 25 nM antimiR-221 or antimiR-Scr in combination with lipofectamine ($n = 3$ hMSC donors). 24 h post-transfection, total RNA including miRNAs was purified as described in the previous paragraph. After confirming effective miR-221 silencing by qRT-PCR, the TruSeq RNA Library prep kit V2 (Illumina) was used to capture poly(A) RNA from 400 ng total RNA. Subsequently cDNA was produced and dual indexed adapters were ligated. The material was amplified by PCR (13 cycles), product size was checked on Labchip GX and product concentration was measured with picogreen. Paired-end sequencing of 2 × 150 bp was performed using the Illumina Novaseq platform to obtain 6GB per sample. Reads were extracted from the raw sequencing data using CASAVA 1.8.2 (Illumina) and aligned to the human reference genome (UCSC's hg19) using the STAR (2.5.0c) splice aware aligner with the gencode v19 transcriptome annotations as additional template. The BAM files were processed using the picard software suite (v1.90) and the Genome Analysis ToolKit (GATK, v3.5). QC metrics were collected at various steps using picard and evaluated along with coverage metrics using GATK. Read counts per exon/gene were then determined by the featureCounts function of the subread package (v1.4.6-p1) using the gencode v19 annotation as markers. The resulting reads were processed using R software (https://cran.r-project.org/) and the DESEQ2 package for NGS analysis. A threshold of 5000 reads per gene was set to filter out low variance genes. Finally, a differential expression (DE) analysis was performed in order to identify the genes that were significantly modulated by antimiR-221 transfection (adjusted p-value ≤ .05).

To evaluate whether the genes significantly upregulated by antimiR-221 transfection included predicted/validated targets of miR-221, a cross-reference analysis with microRNA target databases was performed (miRwalk: http://zmf.umm.uni-heidelberg.de/apps/zmf/mirwalk2/; miRtarBase: http://mirtarbase.mbc.nctu.edu.tw/php/index.php; starBase: http://starbase.sysu.edu.cn/; miRDB: http://mirdb.org/; TargetScan: http://www.targetscan.org/vert_72/). Only genes that were predicted as putative targets of miR-221 by at least three databases were considered.

To identify whether the observed changes in gene expression could be attributed to the modulation of specific upstream regulators, an Ingenuity Pathway Analysis (IPA) (QIAGEN) was performed using the genes significantly modulated by antimiR-221 treatment as input. An IPA z-score ≥ 2.0 and ≤ −2.0 was set for the prediction of activated and inhibited upstream regulators, respectively.

2.8. In vivo osteochondral defect model for endogenous cartilage repair with antimiR-loaded FB/HA hydrogels

An osteochondral biopsy model previously established by our group

[24,25] was adapted for the assessment of endogenous cartilage repair *in vivo*. Briefly, osteochondral biopsies that were 8 mm in diameter and 4 mm in length were produced with a drill from the metacarpal bones of fresh metacarpal-phalangeal joints of 3 to 8 month-old calves obtained from the slaughterhouse. Using a 4 mm-diameter dermal biopsy punch (Stiefel Laboratories, Germany) and a scalpel, osteochondral defects were created by removing the cartilage and part of the subchondral bone. The specimens were incubated overnight in α-MEM medium supplemented with 10% FCS, 1.5 µg/mL fungizone and 50 µg/mL gentamicin to verify sterility. Next, the osteochondral defects were filled with 30 µL FB/HA loaded with 0.04 µg antimiR-221 with or without lipofectamine or FB/HA loaded with 0.4 µg antimiR-221 without lipofectamine. Defects filled with FB/HA only (control) or not filled with hydrogel (empty) were included. The specimens were incubated at 37 °C for 30 min, allowing *in situ* polymerization of the hydrogels.

The osteochondral biopsies were covered with Neuro-Patch membrane (Braun, Germany) to prevent ingrowth of host cell/tissue and implanted subcutaneously on the back of 10 to 14 week old female NMRI nu/nu mouse (Taconic Biosciences) under isoflurane anesthesia.

Before surgery and 6 h after surgery, mice received 0.05 mg/Kg bodyweight of Temgesic (Reckitt Benckiser). During surgery, mice received 9 mg/Kg bodyweight of Ampi-dry (Dopharma). After 4 weeks, the mice were euthanized by cervical dislocation and the osteochondral biopsies were carefully retrieved and fixed in 4% formalin for 1 week. The specimens were then decalcified with 10% ethylenediaminetetraacetic acid (EDTA) for 2 weeks and subsequently embedded in paraffin, sectioned and subjected to histological evaluation. Animal experiments were conducted in the animal facility of the Erasmus MC with approval of the animal ethics committee (under protocol numbers EMC 3284 and **AVD101002016691**).

2.9. Histology and immunohistochemistry

6 µm histological sections of hMSC pellets (sections with the largest pellet area), FB/HA hydrogels and osteochondral biopsies were stained with 0.04% thionine solution (Sigma-Aldrich) in demineralized water to detect glycosaminoglycans (GAGs). Additionally, histological sections of osteochondral biopsies were subjected to
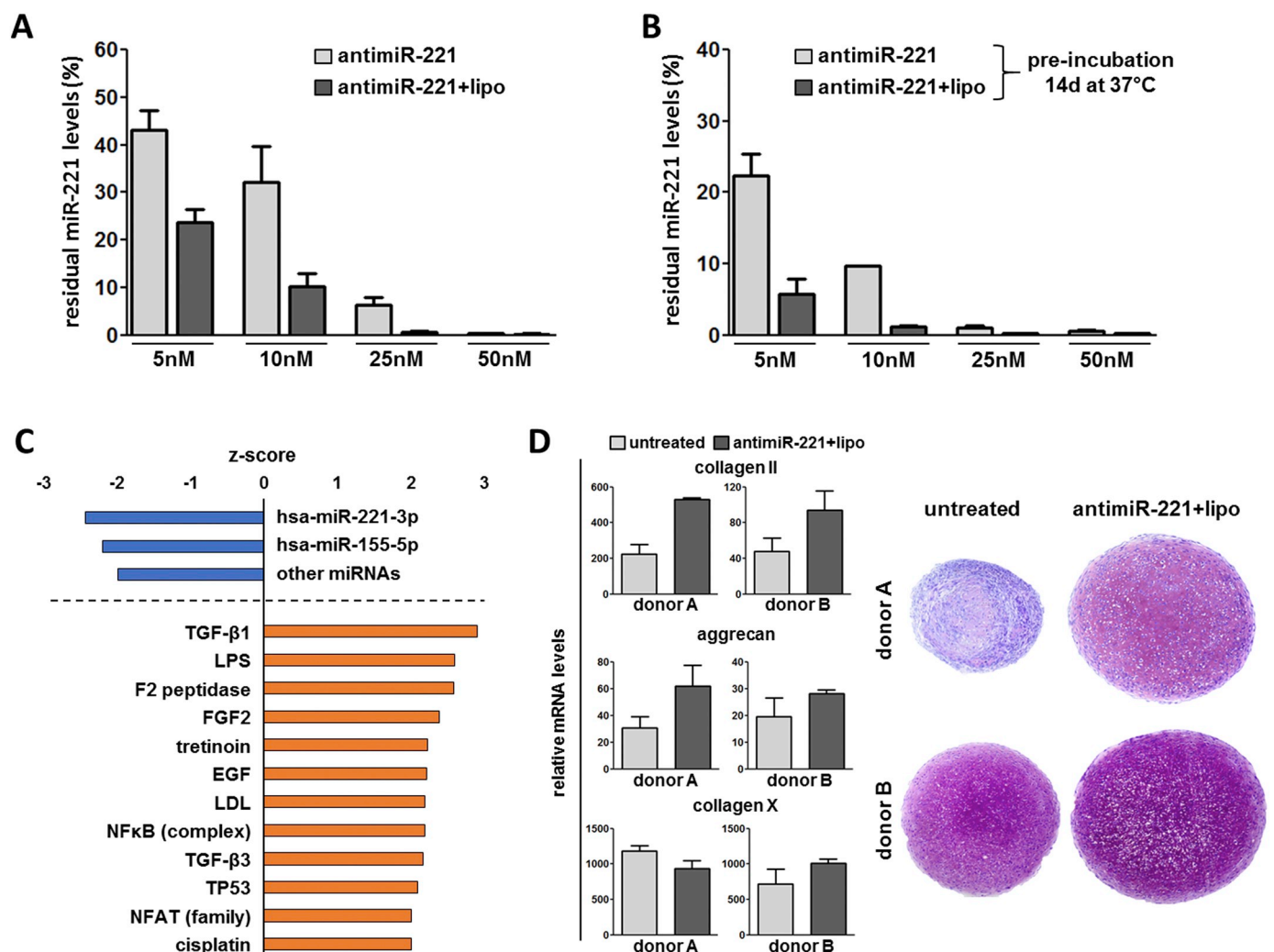

Fig. 1. Effect of antimiR-221 transfection in hMSCs. (A) hMSCs cultured in monolayer were transfected with different concentrations of antimiR-221 alone or with lipofectamine (lipo). After 72 h, miR-221 silencing was determined by qRT-PCR. Data are presented as mean ± SD. (B) To test the stability of the inhibitor, antimiR-221 was pre-incubated at 37 °C for 14 days prior to hMSC transfection. After 72 h, miR-221 silencing was determined by qRT-PCR. Data are presented as mean ± SD. (C) Ingenuity Pathway Analysis (IPA) performed on RNA-seq data identified upstream regulators associated with the changes in gene expression induced by miR-221 silencing 24 h post-transfection. The activation z-score depicts the degree of activation or suppression of a given factor. (D) To evaluate the effect on chondrogenesis, hMSCs were transfected with 25 nM antimiR-221 with lipofectamine and cultured as 3D pellets in chondrogenic medium for 28 days. The mRNA expression of chondrogenesis-related genes was determined by qRT-PCR using HPRT as housekeeping gene. Data are presented as mean ± SD. GAG production and pellet size was evidenced by thionine staining on sections corresponding to the middle of the pellets.

immunohistochemistry for collagen type II. After deparaffinization and rehydration, the sections were enzymatically treated with 1 mg/mL pronase (Sigma-Aldrich) in PBS 1×, followed by treatment with 10 mg/mL hyaluronidase (Sigma-Aldrich) in PBS 1× for antigen retrieval. A primary antibody against collagen type II (mouse anti-human, 1:100 dilution, II-II/II6B3; Developmental Studies Hybridoma Bank) was pre-incubated overnight with a biotin-SP F(ab)2-labelled goat anti-mouse antibody (#115-066-062;Jackson ImmunoResearch Europe) to prevent cross-reaction with mouse antigens; excessive primary antibody was captured by addition of 0.1% normal mouse serum prior to the over-night incubation at 4 °C with the sections. The slides were incubated overnight with the pre-coupled antibodies at 4 °C. Next, an alkaline phosphatase-labelled antibody was used (HK-321-UK, Biogenex Laboratories, CA, USA), which in combination with the Neu Fuchsine substrate resulted in a red staining. An isotype IgG1 monoclonal antibody was used as negative control. Following counterstaining with haematoxilin, the sections were mounted in VectaMount™ AQ mounting medium (Vector Labs, CA, USA). For the quantification of *in vivo* cartilage repair in the osteochondral defect model, thionine positivity in the area of the defect was quantified by a computerised video camera-based image analysis system (NIH, USA ImageJ software, public domain available at: http://rsb.info.nih.gov/nih-image/) under

brightfield microscopy (two replicates per construct). Cartilage repair was expressed as % of thionine-positive area.

2.10. Statistical analysis

For the quantification of cartilage repair in the osteochondral samples, statistically significant differences were determined with IBM SPSS Statistics using a linear mixed model. Differences were considered statistically significant for *p*-values ≤ .05.

3. Results

3.1. Transfection of antimiR-221 into hMSCs leads to inhibition of miR-221 function and stimulation of chondrogenesis

We first aimed to demonstrate that antimiR-221 could be effectively delivered to hMSCs and block miR-221 function. Since LNA oligonucleotides were previously shown to undergo spontaneous internalization by the cells [23], we performed transfection both in the presence and absence of lipofectamine as a carrier. Transfection of antimiR-221 into hMSCs cultured in monolayer led to effective silencing of miR-221 after 72 h, for concentrations of antimiR-221 in the range 5-50 nM

Table 1
RNA-seq analysis of differential gene expression in hMSCs transfected with antimiR-221. hMSCs cultured in monolayer were transfected with antimiR-221 or antimiR-Scr for 24 h, prior to RNA isolation and RNA-seq analysis. The 43 genes found to be significantly modulated by antimiR-221 transfection (adjusted *p*-value (padj) ≤ 0.05) are reported in the table. TGF-β related genes are highlighted in bold.

Gene ID	Gene description	Gene symbol	Fold change	padj	Predicted(P)/validated(V) hsa-miR-221-3p target
ENSG00000119280	Chromosome 1 open reading frame 198	C1orf198	1.8493	3.38E-12	
ENSG00000122376	Shieldin complex subunit 2	SHLD2	2.0606	8.99E-12	
ENSG00000081087	Osteoclastogenesis associated transmembrane protein 1	OSTM1	1.8402	9.56E-10	P
ENSG00000137801	Thrombospondin 1	**THBS1**	1.4707	2.93E-07	V [41]
ENSG00000118523	Cellular communication network factor 2	**CCN2 (CTGF)**	1.5998	9.12E-07	
ENSG00000112096	Superoxide dismutase 2	SOD2	1.5492	1.37E-06	P
ENSG00000149846	Hypoxia up-regulated 1	HYOU1	1.4522	1.78E-06	
ENSG00000119314	Polypyrimidine tract binding protein 3	PTBP3	1.5146	3.93E-06	P
ENSG00000117054	Acyl-CoA dehydrogenase medium chain	ACADM	1.5483	6.82E-06	P
ENSG00000142871	Cellular communication network factor 1	**CCN1 (CYR61)**	1.5121	1.78E-05	
ENSG00000072506	Hydroxysteroid 17-beta dehydrogenase 10	**HSD17B10**	1.5360	7.22E-05	
ENSG00000148677	Ankyrin repeat domain 1	**ANKRD1**	1.7293	5.32E-04	
ENSG00000197965	Myelin protein zero like 1	MPZL1	1.3792	6.52E-04	P
ENSG00000006652	Interferon related developmental regulator 1	**IFRD1**	1.5774	6.87E-04	P
ENSG00000176871	WD repeat and SOCS box containing 2	WSB2	1.3780	6.87E-04	P
ENSG00000136888	ATPase H+ transporting V1 subunit G1	ATP6V1G1	1.3540	1.69E-03	
ENSG00000165617	Dishevelled binding antagonist of beta catenin 1	DACT1	1.5220	2.41E-03	
ENSG00000106484	Mesoderm specific transcript	MEST	1.3437	2.45E-03	
ENSG00000135048	Cell migration inducing hyaluronidase 2	CEMIP2	1.4289	2.63E-03	
ENSG00000106366	Serpin family E member 1	**SERPINE1**	1.3737	3.06E-03	
ENSG00000133816	Microtubule associated monooxygenase, calponin and LIM domain containing 2	**MICAL2**	1.3194	4.89E-03	
ENSG00000168610	Signal transducer and activator of transcription 3	STAT3	1.3180	4.89E-03	
ENSG00000134954	ETS proto-oncogene 1, transcription factor	ETS1	1.3651	6.16E-03	V [42]
ENSG00000075568	Transmembrane protein 131	TMEM131	0.6939	6.18E-03	
ENSG00000125445	Mitochondrial ribosomal protein S7	MRPS7	1.3967	6.71E-03	P
ENSG00000033867	Solute carrier family 4 member 7	SLC4A7	1.3889	7.46E-03	P
ENSG00000178904	dpy-19 like C-mannosyltransferase 3	DPY19L3	1.4131	8.44E-03	
ENSG00000101224	Cell division cycle 25B	CDC25B	0.7231	9.80E-03	
ENSG00000082462	Potassium two pore domain channel subfamily K member 2	KCNK2	1.3322	1.04E-02	P
ENSG00000168374	ADP ribosylation factor 4	**ARF4**	1.2939	1.07E-02	V [43]
ENSG00000114850	Signal sequence receptor subunit 3	SSR3	1.2874	1.10E-02	
ENSG00000117862	Thioredoxin domain containing 12	TXNDC12	1.3584	1.60E-02	
ENSG00000221852	Keratin associated protein 1–5	KRTAP1-5	1.3728	1.69E-02	
ENSG00000104852	Small nuclear ribonucleoprotein U1 subunit 70	**SNRNP70**	0.7612	1.96E-02	
ENSG00000128342	LIF, interleukin 6 family cytokine	**LIF**	1.5151	2.15E-02	
ENSG00000170961	Hyaluronan synthase 2	**HAS2**	1.3339	2.26E-02	
ENSG00000135905	Dedicator of cytokinesis 10	DOCK10	1.3366	2.27E-02	
ENSG00000166224	Sphingosine-1-phosphate lyase 1	SGPL1	1.3507	2.58E-02	
ENSG00000104738	Minichromosome maintenance complex component 4	MCM4	0.7134	3.60E-02	
ENSG00000073182	Fermitin family member 2	**FERMT2**	1.3192	3.95E-02	P
ENSG00000196205	Eukaryotic translation elongation factor 1 alpha 1 pseudogene 5	EEF1A1P5	1.4437	3.96E-02	
ENSG00000099194	Stearoyl-CoA desaturase	**SCD**	1.2899	4.96E-02	P
ENSG00000143183	Transmembrane and coiled-coil domains 1	TMCO1	1.2778	4.99E-02	

(Fig. 1A). In the presence of lipofectamine we achieved a strong miR-221 knockdown (> 99% silencing) for concentrations of antimiR-221 ≥ 25 nM, while a higher dose was required in the case of unassisted transfection (50 nM; Fig. 1A).

Next, to assess the stability of the inhibitor we pre-incubated antimiR-221 in PBS at 37 °C for 14 days, prior to transfection of hMSCs cultured in monolayer. We observed effective miR-221 silencing both in the presence and absence of lipofectamine, suggesting that antimiR-221 remains functional over time (Fig. 1B).

To further investigate the effect of miR-221 silencing in hMSCs, we performed RNA-seq analysis on cells transfected with antimiR-221 for 24 h. We identified 43 significantly modulated genes (Table 1). To determine whether the observed changes in gene expression could be attributed to the modulation of specific upstream regulators, an Ingenuity Pathway Analysis (IPA) was performed using the significantly modulated genes as inputs. "hsa-miR-221-3p" was identified as upstream regulator with the highest z-score of inhibition (Fig. 1C). Furthermore, a cross-reference analysis with microRNA target databases identified 15 upregulated genes in the dataset as putative or experimentally validated targets of miR-221 (Table 1). These data show that transfection of antimiR-221 into hMSCs led to inhibition of miR-221 expression and function, with de-repression of known miR-221 target genes.

We previously demonstrated that miR-221 silencing has a pro-chondrogenic effect in hMSCs [21]. Interestingly, the IPA analysis indicated "TGF-β1" as upstream regulator with the highest z-score of activation (Fig. 1C), and 14 TGF-β related genes were found to be significantly modulated by miR-221 silencing (Table 1, genes in bold). When hMSCs transfected with antimiR-221 were cultured as 3D pellets, miR-221 silencing led to increased mRNA expression of collagen II but not of collagen X, in addition to increased aggrecan mRNA expression in a donor-dependent manner (Fig. 1D). Thionine staining evidenced enhanced GAG production in hMSCs transfected with antimiR-221 (Fig. 1D).

Altogether, our data indicate that transfection of antimiR-221 into hMSCs effectively blocks miR-221 function and enhances their chondrogenic potential.

3.2. FB/HA hydrogels enable effective cell transfection and knockdown of miR-221 in situ

We aimed to develop a hydrogel-based system for delivering antimiR-221 to endogenous cells and inducing miR-221 knockdown in situ. We selected a FB/HA conjugate hydrogel that is particularly promising for cartilage repair applications in vivo [22,26], and already

clinically approved as a medical device (Regenogel™) for the local treatment of osteoarthritis.

We first investigated whether FB/HA provided a favourable environment for cell transfection with antimiR-221. FB/HA hydrogels were loaded with antimiR-221/lipofectamine and hMSCs immediately prior to polymerization induced by thrombin, and the hydrogels were cultured in vitro for 7 days. qRT-PCR analysis demonstrated effective miR-221 knockdown, with a dose-dependent effect for concentrations of antimiR-221 in the range 25–250 nM (Fig. 2A).

Flow cytometry analysis showed that a high percentage of cells were transfected with antimiR-221 already after 3 days of culture in FB/HA loaded with antimiR-221 (~80% for 50 nM antimiR-221; Fig. 2B). Importantly, cell viability in the hydrogels was not affected by the presence of antimiR-221 or lipofectamine up to 14 days of culture (Fig. S1). Thus, FB/HA provides a supportive environment for cell transfection with antimiR-221.

To determine whether FB/HA could potentially retain antimiR-221 when applied in an osteochondral defect to transduce cells that invade the matrix over time, we next assessed the release profile of the inhibitor from the hydrogel. As shown in Fig. 3A, FB/HA retained most of the antimiR-221/lipofectamine complexes over 14 days of in vitro culture. Dissolution of the hydrogels at day 14 confirmed that > 85% of the antimiR-221 was still present in the gel (Fig. 3B). When FB/HA was loaded with antimiR-221 without lipofectamine carrier, the release of the inhibitor was faster (Fig. 3A). Nevertheless, ~50% of the inhibitor was still retained by FB/HA after 14 days (Fig. 3B). These data indicate that FB/HA retains antimiR-221 over time, with or without a carrier, and provides a supportive environment for hMSC transfection. Interestingly, these findings were not unique for FB/HA, as comparable results were obtained when a collagen I hydrogel was used (Fig. S2).

Next, in order to mimic the process of transfection of endogenous cells that migrate into a hydrogel, hMSCs were seeded on the surface of FB/HA hydrogels loaded with antimiR-221 with or without lipofectamine, and allowed to infiltrate the constructs. As shown in Fig. 3C, qRT-PCR analysis performed after 7 days of culture demonstrated effective inhibition of miR-221. While miR-221 knockdown was particularly strong in the presence of lipofectamine (> 99%), even in the case of unassisted transfection a silencing efficiency of 60% to 80% was achieved for concentrations of antimiR-221 in the range 50-250 nM. Loading of FB/HA with a scrambled antimiR molecule had no effect on miR-221 levels, confirming that inhibition of miR-221 by antimiR-221 was specific (Fig. 3C).

Finally, we assessed antimiR-221 stability in the hydrogels by pre-culturing FB/HA loaded with 250 nM antimiR-221 for 14 days at 37 °C prior to hMSC seeding. The constructs were still capable of inducing
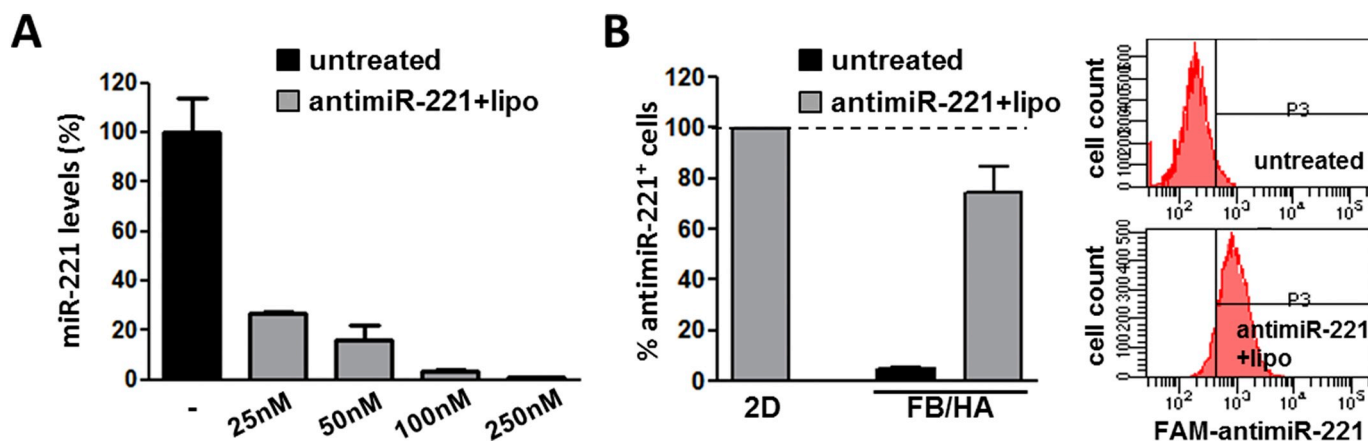

Fig. 2. FB/HA conjugate hydrogel supports transfection of antimiR-221 into hMSCs. (A) hMSCs were cultured in FB/HA hydrogels loaded with different concentrations of antimiR-221 with lipofectamine. miR-221 silencing was determined by qRT-PCR at day 7 and data are presented as mean ± SD. (B) hMSCs were cultured in FB/HA hydrogels loaded with 50 nM FAM-labelled antimiR-221 with lipofectamine. After 3 days, hMSCs were retrieved and analyzed by flow cytometry to quantify the transfection efficiency (2D = monolayer positive control). Data are presented as mean ± SD.
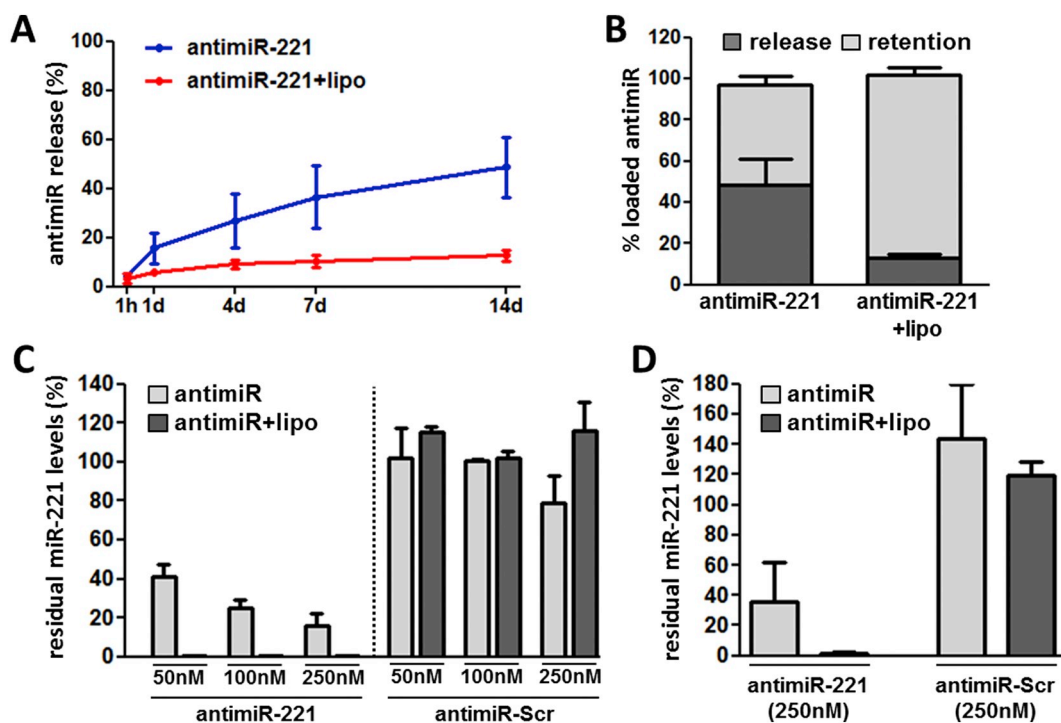
Fig. 3. Validation of antimiR-221 loaded FB/HA as delivery system for cell transfection *in situ*. (A) FB/HA hydrogels were loaded with FAM-labelled antimiR-221 alone or with lipofectamine. The cumulative release of antimiR-221 was determined by measuring the concentration of antimiR-221 in the releasates. (B) The histogram depicts the % of antimiR-221 release and retention at the end-point (day 14). Data are presented as mean ± SD. (C) hMSCs were seeded on the surface of FB/HA hydrogels loaded with different concentrations of antimiR-221 or antimiR-Scr alone or with lipofectamine, and allowed to infiltrate the constructs. After 7 days, miR-221 silencing was determined by qRT-PCR. Data are presented as mean ± SD. (D) FB/HA hydrogels loaded with antimiR-221 or antimiR-Scr alone or with lipofectamine were pre-incubated at 37 °C for 14 days, prior to hMSC seeding on the surface of the hydrogels. miR-221 silencing was determined by qRT-PCR 7 days post-seeding. Data are presented as mean ± SD.

miR-221 silencing, confirming that antimiR-221 retained by FB/HA remains functional for a period of at least 2–3 weeks (Fig. 3D). A comparison between pre-cultured and freshly prepared hydrogels (Fig. 3D and C, respectively) indicated no difference in miR-221 silencing for lipofectamine-assisted transfection (from 99.7% to 98.5%), and a small decrease for unassisted transfection (from 84.3% to 64.1%), likely due to the faster release of the inhibitor.

Taken together, our data show that FB/HA hydrogel loaded with antimiR-221 represents a suitable delivery system for the transfection of endogenous cells. While carrier-assisted transfection enhanced the potency of the system, even in the absence of a carrier FB/HA hydrogels retained antimiR-221 overtime and induced miR-221 silencing in hMSCs *in situ*.

3.3. FB/HA hydrogels loaded with antimiR-221/lipofectamine enhance endogenous cartilage repair in vivo

To assess the effect of antimiR-221 delivery by FB/HA on endogenous joint-resident cells, we employed an *in vivo* model that simulates an osteochondral defect [21,27]. While we previously investigated the chondrogenic potential of *in vitro* cultured cells loaded in different hydrogels, we now exploited the osteochondral model to recapitulate the endogenous cartilage repair process.

We first confirmed that FB/HA supported chondrogenesis of progenitor cells by embedding bone marrow-derived hMSCs in the hydrogel and culturing in chondrogenic medium *in vitro* (Fig. S3A). Next, osteochondral defects were created in bovine osteochondral biopsies and filled with FB/HA only (control) or FB/HA loaded with 0.04 μg antimiR-221 (250 nM concentration) with or without lipofectamine (Fig. 4A). Since unassisted transfection proved overall less effective *in vitro*, a higher dose of 0.4 μg antimiR-221 without lipofectamine was also included. Defects not filled with the hydrogel (empty) were

included as negative control condition (Fig. S3B). The constructs were implanted subcutaneously in nude mice and retrieved after 4 weeks to evaluate the potency of the system to induce cartilage repair. As shown in Fig. 4B, all hydrogel conditions proved favourable for the invasion of endogenous cells, their differentiation into chondrocytes, and the production of repair cartilage within the osteochondral defects. However, we observed some variability in endogenous cell infiltration, with ~20% of the specimens showing limited cell invasion (an example is shown in Fig. S3C).

To determine whether delivery of antimiR-221 to endogenous cells improved cartilage repair, we quantified the thionine-positive area in the osteochondral defects (Fig. 4C). Since our approach of *in situ* transfection of endogenous cells relies on good cellular invasion, we excluded from the analysis the specimens with limited cell infiltration (shown as grey circles in Fig. 4C). In the case of unassisted transfection, the lower antimiR-221 dose led to a slight increase in the amount of repair cartilage, that did not reach statistical significance. Only 2 of the 5 specimens showed increased cartilage production in comparison to control hydrogels, suggesting a certain degree of variability in the efficacy of *in vivo* unassisted transfection. When lipofectamine was used as a carrier, loading of FB/HA with antimiR-221 enhanced cartilage repair by endogenous cells, with a significant 2-fold increase in the amount of repair cartilage (Fig. 4B–C).

Immunohistochemical analysis of the constructs evidenced abundant production of the hyaline cartilage marker collagen II within the newly-formed tissue, particularly in the case of FB/HA loaded with antimiR-221/lipofectamine (Fig. 4B).

In conclusion, our data demonstrate that delivery of antimiR-221 to endogenous cells by a suitable hydrogel material significantly enhanced cartilage repair by endogenous cells *in vivo*. The effect was particularly evident in the presence of lipofectamine as a carrier, that likely increased the effectiveness of *in vivo* transfection.
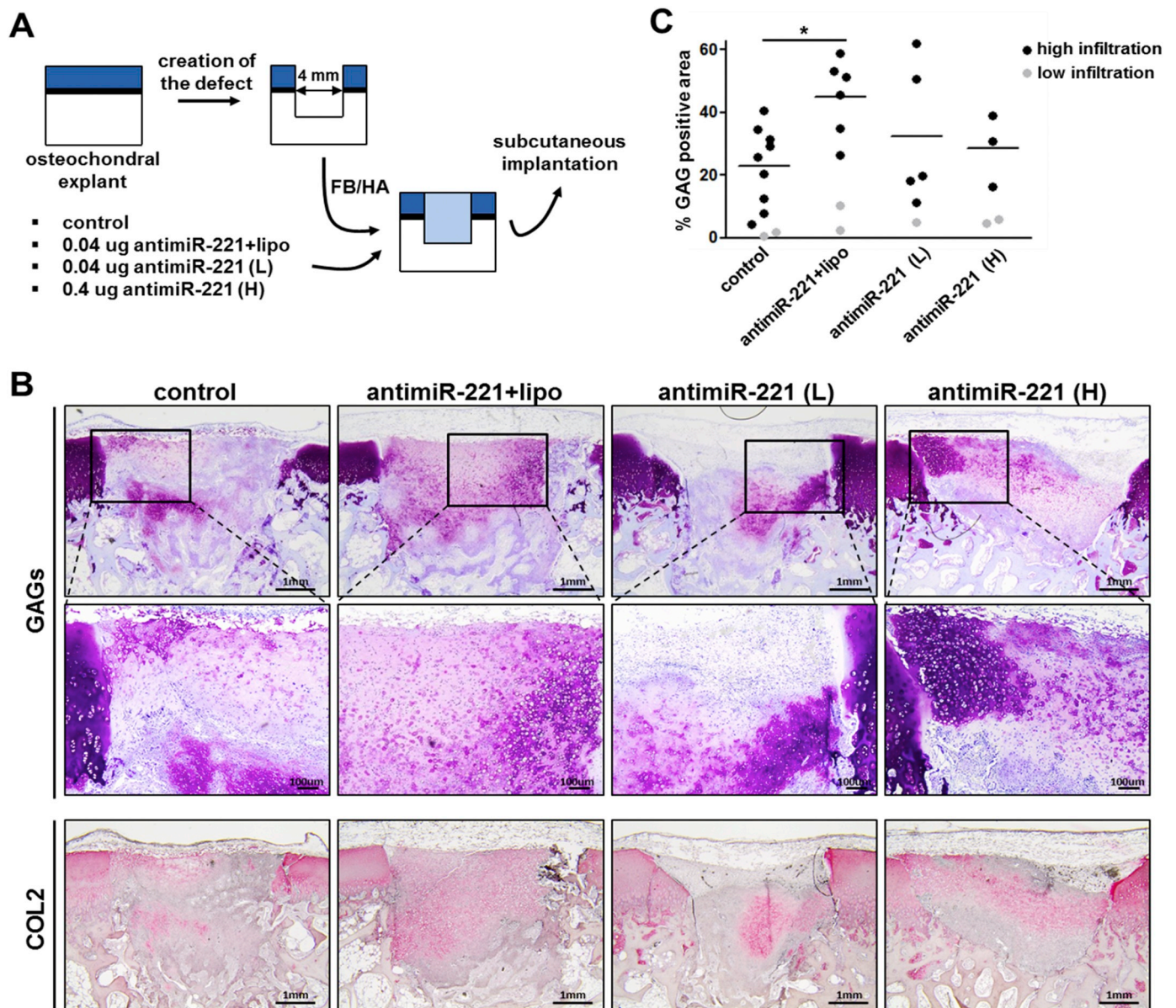
Fig. 4. Effect of antimiR-221 loaded FB/HA hydrogels on endogenous cartilage repair *in vivo*. (A) Osteochondral defects (Ø 4 mm) were produced in bovine osteochondral biopsies and filled with FB/HA hydrogels loaded with the indicated doses of antimiR-221 with or without lipofectamine, performing *in situ* polymerization (L = low dose; H = high dose). The constructs were implanted subcutaneously in nude mice for 4 weeks. (B) Newly-formed cartilage in the osteochondral defects was evidenced by thionine staining and collagen II production was evidenced by immunohistochemistry. Representative sections are shown. (C) Cartilage repair was quantified by measuring the % of the osteochondral defects filled with thionine-positive repair cartilage. Data are presented as dot plot with average values. Statistical significance was determined using a linear mixed model (*p < .05).

4. Discussion

In this study, we demonstrated that implantation of an antimicroRNA-loaded hydrogel in osteochondral defects significantly enhanced cartilage production by endogenous cells. miR-221 was selected as candidate microRNA based on our previous studies [20,21], and was here validated as a potential target to guide endogenous cartilage repair *in vivo*. To the best of our knowledge, our findings provide first indication that hydrogel-assisted antimicroRNA delivery may serve as a novel approach to stimulate endogenous cartilage repair.

Our work strongly supports the idea of targeting anti-chondrogenic factors to guide cartilage repair. The research on novel strategies for cartilage repair has so far focused almost exclusively on the stimulation of cartilage anabolism, especially *via* growth factor therapy. Despite the hype surrounding such preparations, their effectiveness is still debated

and a lack of standardization is limiting their clinical use [28,29]. Interestingly, endogenous anabolic stimuli in the joint may be already sufficient for cartilage repair, as indicated by the spontaneous formation of cartilaginous tissue following microfracture. However, the fact that cartilage repair is often impaired by insufficient production or degeneration of the repair tissue suggests the presence of anti-chondrogenic factors in the joint environment that counteract regeneration. In this regard, a number of anti-chondrogenic regulators, including microRNAs, have been characterized, and a growing body of evidence indicates that targeting these factors may "release the brakes" and create better conditions to achieve optimal cartilage repair (reviewed in [30,31]). This is further confirmed by the outcome of our study, that validates miR-221 as target to enhance the chondro-regenerative potential of endogenous cells. While the molecular mechanism supporting the pro-chondrogenic effect of miR-221 silencing remains to be

determined, our data suggest that an interplay between miR-221 and the TGF-β signaling may be implicated.

Our strategy is based on the manipulation of endogenous cells *via* non-viral transfection of an antimiR oligonucleotide. Non-viral carriers are a preferable choice for translational research, being safer and cheaper [32]. Furthermore, they can serve as a minimally invasive mean to trigger a regenerative response, while allowing the host tissues to gradually take over tissue repair. Here we loaded antimiR-221 into a FB/HA hydrogel, in combination with lipofectamine as state-of-the-art non-viral carrier, or without carrier to evaluate unassisted transfection. While lipofectamine-mediated transfection performed better in all experiments, both strategies led to efficient cell transfection and miR-221 silencing *in situ*. This was likely favored by the existence of an interaction between antimiR-221 or lipofectamine and FB/HA, as indicated by the high retention of functional inhibitor over a period of weeks. These findings are consistent with recent studies that showed co-localization of LNA-oligonucleotides and fibrin fibers within different hydrogels [33,34]. Interestingly, this approach may also be applied to different biomaterials, as demonstrated by our results obtained with a collagen I hydrogel. Further studies are needed to elucidate the exact nature of the interactions between hydrogels and LNA-oligonucleotides, since manipulation of the material properties may allow to alter the release profile as desired. Finally, it will be important to investigate whether differences in the release profile may arise *in vivo* due to the presence of cells and biological fluids.

AntimiR-221 was found to transfect progenitor cells and inhibit miR-221 expression *in vitro* both with and without the use of lipofectamine carrier. When antimiR-221 loaded FB/HA hydrogels were implanted in an osteochondral defect model, however, only carrier-assisted transfection led to a significant increase in endogenous cartilage repair. We hypothesize that a lower antimiR-221 retention and transfection efficiency in the absence of the carrier made it challenging to observe a clear biological effect. The large differences in cartilage repair observed in these specimens may reflect a high variability in the effectiveness of *in vivo* unassisted transfection. Interestingly, increasing the antimiR-221 dose did not lead to further improvements, suggesting that a higher local concentration of the inhibitor (at least in the early phase post-implantation) did not compensate for a reduced transfection efficiency. These findings provide valuable directions for future work, that should focus on the optimization of the hydrogel formulation (*e.g.* FB/HA ratio and amount of crosslinking) to identify conditions that may increase antimiR retention and/or transfection efficiency.

Of note, the process of endogenous cartilage repair is only partially understood and the specific contribution of different progenitor/stem cell populations has not yet been elucidated. Full-thickness cartilage lesions induce blood clot formation, invasion of multipotent cells and fibrocartilage production. In 1993, Shapiro et al. attributed endogenous cartilage repair to bone marrow cells by radiolabeling [7]. It is now clear that bone marrow is not the only tissue involved, and various progenitor cell populations contribute to endogenous cartilage repair, *e.g.* cells from synovium and the surface zone of articular cartilage [35]. A recent study demonstrated that the progenitor cells involved in articular cartilage repair are predominantly of the GDF5-lineage, and these cells reside in the synovium, subchondral bone marrow and articular cartilage [36]. Unfortunately, an in-depth investigation of the precise cellular and molecular events still lacks. While this "knowledge gap" should not discourage the development of tools for endogenous cartilage repair, it would be of major relevance for establishing targeted approaches directed towards specific cell populations. Importantly, the pro-chondrogenic effect of antimiR-221 is not restricted to a specific progenitor cell source, as indicated by the results obtained with fetal umbilical cord and adult bone marrow hMSCs [21], as well as dedifferentiated intervertebral disc cells [37]. This versatility likely relates to the targeting of miR-221 as a crucial anti-chondrogenic regulator that inhibits chondrogenesis in progenitor cells of various origin. Our current work further supports this concept and leads us to speculate

that an antimiR-221 based approach could potentially target any source of chondro-progenitor cells invading the osteochondral defect.

In this work we did not focus on the issue of stimulating the proliferation and recruitment of endogenous cells. The bovine osteochondral model displayed an overall high rate of endogenous cell infiltration, likely favored by the young age of the animals and the healthy state of the joint. However, ~20% of the constructs exhibited limited rate of endogenous cell ingrowth and had to be excluded from the analysis. It is likely that in the context of an osteochondral lesion, the rate of endogenous cell invasion is impacted by several factors, including patient specific characteristics. To address this need, few studies have succeeded in loading proliferative and/or chemotactic factors in scaffolds to enhance the recruitment of endogenous cells to the lesion. Collagen I scaffold containing stromal cell-derived factor 1 were employed to enhance endogenous repair of partial-thickness defects in rabbits [38]. TGF-β3 and mechano growth factor-functionalized silk fibroin scaffolds enhanced endogenous cell recruitment and *in situ* articular cartilage regeneration in a rabbit model [39]. In addition to the use of chemokines, employing materials with properties that are particularly favourable for endogenous cell infiltration, adhesion and survival may significantly impact endogenous repair. A number of material features such as surface chemistry, micro/nanotopography and matrix stiffness can exert a profound influence on cell behavior [40]. These parameters should be carefully taken into account and properly modified to enhance the "cell colonizing properties" of the biomaterial. In this view, our antimiR-221 based system could be implemented with chemotactic factors and/or modified biomaterial properties to further extend its application to situations where endogenous cell infiltration is expected to be limited.

Our results were obtained using a bovine osteochondral biopsy model to study cartilage repair in a simulated osteochondral defect *in vivo*. Also in consideration of previous work [21,27], this proved as a valuable strategy to investigate early events involved in cartilage repair, including the attraction of endogenous cells, their differentiation into chondrocytes and cartilage matrix production. The model also has limitations, related to its ectopic nature and the absence of proper mechanical forces. Future development of our approach will require validation studies in the context of orthotopic osteochondral defects in large size animals. Importantly, this will allow to investigate the mechanical properties and the long-term stability of the repair cartilage generated by antimiR-221 treatment, and may pave the way for potential applications.

5. Conclusions

In conclusion, this study established a novel non-invasive FB/HA hydrogel-based approach that exploits antimicroRNA therapy to enhance endogenous repair of osteochondral defects. This system is highly versatile and may be easily adapted for the use of different biomaterials or for targeting alternative inhibitors of tissue repair. In addition, our work may contribute to further development of microRNA therapy for tissues where biomaterial-driven manipulation of microRNAs has shown significant therapeutic potential, including cartilage, bone, heart and nervous system. We hope that our findings will give further impulse to these fields, pushing in the direction of translational research on microRNA therapy for tissue repair.

Author contributions

A.L.: study conception and experimental design, data collection, analysis and interpretation, manuscript writing; K.S.: experimental design, flow cytometry data collection and analysis; L.V.: assistance with animal experiments and histological data collection; J.O.: RNA-seq data analysis and interpretation; N.K.: assistance with animal experiments and histological data collection; A.Y.: experimental design, data interpretation; G.O.: study conception and experimental design, data

interpretation, manuscript writing. All authors have read, revised and approved the final submitted work.

Acknowledgements

Appendix A. Supplementary data

Supplementary data to this article can be found online at https://doi.org/10.1016/j.jconrel.2019.07.040.

References

[1] M. Brittberg, D. Recker, J. Ilgenfritz, D.B.F. Saris, S.E.S. Group, Matrix-applied characterized autologous cultured chondrocytes versus microfracture: five-year follow-up of a prospective randomized trial, Am. J. Sports Med. 46 (2018) 1343–1351.
[2] T.S. de Windt, L.A. Vonk, I.C. Slaper-Cortenbach, M.P. van den Broek, R. Nizak, M.H. van Rijen, R.A. de Weger, W.J. Dhert, D.B. Saris, Allogeneic mesenchymal stem cells stimulate cartilage regeneration and are safe for single-stage cartilage repair in humans upon mixture with recycled autologous chondrons, Stem Cells 35 (2017) 256–264.
[3] Y.G. Koh, O.R. Kwon, Y.S. Kim, Y.J. Choi, D.H. Tak, Adipose-derived mesenchymal stem cells with microfracture versus microfracture alone: 2-year follow-up of a prospective randomized trial, Arthroscopy 32 (2016) 97–109.
[4] I. Akgun, M.C. Unlu, O.A. Erdal, T. Ogut, M. Erturk, E. Ovali, F. Kantarci, G. Caliskan, Y. Akgun, Matrix-induced autologous mesenchymal stem cell implantation versus matrix-induced autologous chondrocyte implantation in the treatment of chondral defects of the knee: a 2-year randomized study, Arch. Orthop. Trauma Surg. 135 (2015) 251–263.
[5] W. Wei, J. Luo, Thoughts on chemistry, manufacturing, and control of cell therapy products for clinical application, Hum. Gene Ther. (2018), https://doi.org/10.1089/hgt.2018.097.
[6] J.R. Steadman, W.G. Rodkey, S.B. Singleton, K.K. Briggs, Microfracture technique for full-thickness chondral defects: technique and clinical results, Oper. Tech. Orthop. 7 (1997) 300–304.
[7] F. Shapiro, S. Koide, M.J. Glimcher, Cell origin and differentiation in the repair of full-thickness defects of articular cartilage, J. Bone Joint Surg. Am. 75 (1993) 532–553.
[8] E.B. Hunziker, L.C. Rosenberg, Repair of partial-thickness defects in articular cartilage: cell recruitment from the synovial membrane, J. Bone Joint Surg. Am. 78 (1996) 721–733.
[9] P.C. Kreuz, M.R. Steinwachs, C. Erggelet, S.J. Krause, G. Konrad, M. Uhl, N. Sudkamp, Results after microfracture of full-thickness chondral defects in different compartments in the knee, Osteoarthr. Cartil. 14 (2006) 1119–1125.
[10] J.P. Benthien, P. Behrens, Autologous matrix-induced chondrogenesis (AMIC): combining microfracturing and a collagen I/III matrix for articular cartilage resurfacing, Cartilage 1 (2010) 65–68.
[11] W.D. Stanish, R. McCormack, F. Forriol, N. Mohtadi, S. Pelet, J. Desnoyers, A. Restrepo, M.S. Shive, Novel scaffold-based BST-CarGel treatment results in superior cartilage repair compared with microfracture in a randomized controlled trial, J. Bone Joint Surg. Am. 95 (2013) 1640–1650.
[12] X. Zhang, Y. Li, Y.E. Chen, J. Chen, P.X. Ma, Cell-free 3D scaffold with two-stage delivery of miRNA-26a to regenerate critical-sized bone defects, Nat. Commun. 7 (2016) 10376.
[13] R.M. Raftery, I. Mencia Castano, G. Chen, B. Cavanagh, B. Quinn, C.M. Curtin, S.A. Cryan, F.J. O'Brien, Translating the role of osteogenic-angiogenic coupling in bone formation: highly efficient chitosan-pDNA activated scaffolds can accelerate bone regeneration in critical-sized bone defects, Biomaterials 149 (2017) 116–127.
[14] M. Monaghan, S. Browne, K. Schenke-Layland, A. Pandit, A collagen-based scaffold delivering exogenous microrna-29B to modulate extracellular matrix remodeling, Mol. Ther. 22 (2014) 786–796.
[15] C.M. Curtin, I.M. Castano, F.J. O'Brien, Scaffold-based microRNA therapies in regenerative medicine and cancer, Adv. Healthc. Mater. 7 (2017).
[16] A. Martinez-Sanchez, K.A. Dudek, C.L. Murphy, Regulation of human chondrocyte function through direct inhibition of cartilage master regulator SOX9 by microRNA-145 (miRNA-145), J. Biol. Chem. 287 (2012) 916–924.
[17] B. Yang, H. Guo, Y. Zhang, L. Chen, D. Ying, S. Dong, MicroRNA-145 regulates chondrogenic differentiation of mesenchymal stem cells by targeting Sox9, PLoS One 6 (2011) e21679.
[18] S. Miyaki, T. Sato, A. Inoue, S. Otsuki, Y. Ito, S. Yokoyama, Y. Kato, F. Takemoto, T. Nakasa, S. Yamashita, S. Takada, M.K. Lotz, H. Ueno-Kudo, H. Asahara, MicroRNA-140 plays dual roles in both cartilage development and homeostasis, Genes Dev. 24 (2010) 1173–1185.
[19] M. Yoshizuka, T. Nakasa, Y. Kawanishi, S. Hachisuka, T. Furuta, S. Miyaki, N. Adachi, M. Ochi, Inhibition of microRNA-222 expression accelerates bone healing with enhancement of osteogenesis, chondrogenesis, and angiogenesis in a rat refractory fracture model, J. Orthop. Sci. 21 (2016) 852–858.
[20] A. Lolli, E. Lambertini, L. Penolazzi, M. Angelozzi, C. Morganti, T. Franceschetti, S. Pelucchi, R. Gambari, R. Piva, Pro-chondrogenic effect of miR-221 and slug depletion in human MSCs, Stem Cell Rev. 10 (2014) 841–855.
[21] A. Lolli, R. Narcisi, E. Lambertini, L. Penolazzi, M. Angelozzi, N. Kops, S. Gasparini, G.J. van Osch, R. Piva, Silencing of antichondrogenic microRNA-221 in human mesenchymal stem cells promotes cartilage repair in vivo, Stem Cells 34 (2016) 1801–1811.
[22] Z. Li, K.M. Kaplan, A. Wertzel, M. Peroglio, B. Amit, M. Alini, S. Grad, A. Yayon, Biomimetic fibrin-hyaluronan hydrogels for nucleus pulposus regeneration, Regen. Med. 9 (2014) 309–326.
[23] C.A. Stein, J.B. Hansen, J. Lai, S. Wu, A. Voskresenskiy, A. Hog, J. Worm, M. Hedtjarn, N. Souleimanian, P. Miller, H.S. Soifer, D. Castanotto, L. Benimetskaya, H. Orum, T. Koch, Efficient gene silencing by delivery of locked nucleic acid antisense oligonucleotides, unassisted by transfection reagents, Nucleic Acids Res. 38 (2010) e3.
[24] M.L. de Vries-van Melle, R. Narcisi, N. Kops, W.J. Koevoet, P.K. Bos, J.M. Murphy, J.A. Verhaar, P.M. van der Kraan, G.J. van Osch, Chondrogenesis of mesenchymal stem cells in an osteochondral environment is mediated by the subchondral bone, Tissue Eng. Part A 20 (2014) 23–33.
[25] M.L. de Vries-van Melle, E.W. Mandl, N. Kops, W.J. Koevoet, J.A. Verhaar, G.J. van Osch, An osteochondral culture model to study mechanisms involved in articular cartilage repair, Tissue Eng. Part C Methods 18 (2012) 45–53.
[26] M. Peeters, S.E. Detiger, L.S. Karfeld-Sulzer, T.H. Smit, A. Yayon, F.E. Weber, M.N. Helder, BMP-2 and BMP-2/7 heterodimers conjugated to a fibrin/hyaluronic acid hydrogel in a large animal model of mild intervertebral disc degeneration, Biores. Open Access 4 (2015) 398–406.
[27] M.L. de Vries-van Melle, M.S. Tihaya, N. Kops, W.J. Koevoet, J.M. Murphy, J.A. Verhaar, M. Alini, D. Eglin, G.J. van Osch, Chondrogenic differentiation of human bone marrow-derived mesenchymal stem cells in a simulated osteochondral environment is hydrogel dependent, Eur. Cell Mater. 27 (2014) 112–123 (discussion 123).
[28] J. Chahla, C.S. Dean, G. Moatshe, C. Pascual-Garrido, R. Serra Cruz, R.F. LaPrade, Concentrated bone marrow aspirate for the treatment of chondral injuries and osteoarthritis of the knee: a systematic review of outcomes, Orthop. J. Sports Med. 4 (2016) 2325967115625481.
[29] G. Moatshe, E.R. Morris, M.E. Cinque, C. Pascual-Garrido, J. Chahla, L. Engebretsen, R.F. Laprade, Biological treatment of the knee with platelet-rich plasma or bone marrow aspirate concentrates, Acta Orthop. 88 (2017) 670–674.
[30] A. Lolli, F. Colella, C. De Bari, G. van Osch, Targeting anti-chondrogenic factors for the stimulation of chondrogenesis: a new paradigm in cartilage repair, J. Orthop. Res. 37 (1) (2018) 12–22.
[31] A. Lolli, L. Penolazzi, R. Narcisi, G. van Osch, R. Piva, Emerging potential of gene silencing approaches targeting anti-chondrogenic factors for cell-based cartilage repair, Cell. Mol. Life Sci. 74 (2017) 3451–3465.
[32] S. Raisin, E. Belamie, M. Morille, Non-viral gene activated matrices for mesenchymal stem cells based tissue engineering of bone and cartilage, Biomaterials 104 (2016) 223–237.
[33] P.M.D. Moreno, A.R. Ferreira, D. Salvador, M.T. Rodrigues, M. Torrado, E.D. Carvalho, U. Tedebark, M.M. Sousa, I.F. Amaral, J. Wengel, A.P. Pego, Hydrogel-assisted antisense LNA Gapmer delivery for in situ gene silencing in spinal cord injury, Mol. Ther. Nucleic Acids 11 (2018) 393–406.
[34] J.P. Garcia, J. Stein, Y. Cai, F. Riemers, E. Wexselblatt, J. Wengel, M. Tryfonidou, A. Yayon, K.A. Howard, L.B. Creemers, Fibrin-hyaluronic acid hydrogel-based delivery of antisense oligonucleotides for ADAMTS5 inhibition in co-delivered and resident joint cells in osteoarthritis, J. Control. Release 294 (2019) 247–258.
[35] G.I. Im, Endogenous cartilage repair by recruitment of stem cells, Tissue Eng. Part B Rev. 22 (2016) 160–171.
[36] A.J. Roelofs, J. Zupan, A.H.K. Riemen, K. Kania, S. Ansboro, N. White, S.M. Clark, C. De Bari, Joint morphogenetic cells in the adult mammalian synovium, Nat. Commun. 8 (2017) 15040.
[37] L. Penolazzi, E. Lambertini, L.S. Bergamin, J. Roncada, P. De Bonis, M. Cavallo, R. Piva, MicroRNA-221 silencing attenuates the degenerated phenotype of intervertebral disc cells, Aging (Albany NY) 10 (2018) 2001–2015.
[38] W. Zhang, J. Chen, J. Tao, Y. Jiang, C. Hu, L. Huang, J. Ji, H.W. Ouyang, The use of type 1 collagen scaffold containing stromal cell-derived factor-1 to create a matrix environment conducive to partial-thickness cartilage defects repair, Biomaterials 34 (2013) 713–723.

[39] Z. Luo, L. Jiang, Y. Xu, H. Li, W. Xu, S. Wu, Y. Wang, Z. Tang, Y. Lv, L. Yang, Mechano growth factor (MGF) and transforming growth factor (TGF)-beta3 functionalized silk scaffolds enhance articular hyaline cartilage regeneration in rabbit model, Biomaterials 52 (2015) 463–475.

[40] M. Ventre, P.A. Netti, Engineering cell instructive materials to control cell fate and functions through material cues and surface patterning, ACS Appl. Mater. Interfaces 8 (2016) 14896–14908.

[41] S. Farberov, R. Meidan, Fibroblast growth factor-2 and transforming growth factor-beta1 oppositely regulate miR-221 that targets thrombospondin-1 in bovine luteal endothelial cells, Biol. Reprod. 98 (2018) 366–375.

[42] J. Xu, Y. Liu, M. Deng, J. Li, H. Cai, Q. Meng, W. Fang, X. Long, J. Ke, MicroRNA221-3p modulates Ets-1 expression in synovial fibroblasts from patients with osteoarthritis of temporomandibular joint, Osteoarthr. Cartil. 24 (2016) 2003–2011.

[43] Q. Wu, X. Ren, Y. Zhang, X. Fu, Y. Li, Y. Peng, Q. Xiao, T. Li, C. Ouyang, Y. Hu, Y. Zhang, W. Zhou, W. Yan, K. Guo, W. Li, Y. Hu, X. Yang, G. Shu, H. Xue, Z. Wei, Y. Luo, G. Yin, MiR-221-3p targets ARF4 and inhibits the proliferation and migration of epithelial ovarian cancer cells, Biochem. Biophys. Res. Commun. 497 (2018) 1162–1170.